Elements Located Upstream and Downstream of the Major Splice Donor Site Influence the Ability of HIV-2 Leader RNA To Dimerize *in Vitro*†

Jean-Marc Lanchy, Casey A. Rentz, John D. Ivanovitch, and J. Stephen Lodmell*

Division of Biological Sciences, The University of Montana, Missoula, Montana 59812

Received November 6, 2002; Revised Manuscript Received December 19, 2002

ABSTRACT: An essential step in the replication cycle of all retroviruses is the dimerization of genomic RNA prior to or during budding and maturation of the viral particle. In HIV-1, a 5′ leader region site termed stem−loop 1 (SL1) promotes RNA dimerization *in vitro* and influences dimerization *in vivo*. In HIV-2, two sequences promote dimerization of RNA fragments *in vitro*: the 5′-end of the primer-binding site (PBS) and a stem−loop region homologous to the HIV-1 SL1 sequence. Because HIV-2 RNA constructs of different lengths use these two dimerization signals disproportionately, we hypothesized that other sequences could modulate their relative utilization. Here, we characterized the influence of sequences upstream and downstream of the major splice donor site on the formation of HIV-2 RNA dimers *in vitro* using a variety of RNA constructs and dimerization and electrophoresis protocols. We first assayed the formation of loose or tight dimers for 1−444 and 1−561 model RNAs. Although both RNAs could form PBS-dependent loose dimers, the 1−561 RNA was unable to make SL1-dependent tight dimers. Using RNAs truncated at their 5′- and/or 3′-ends and by making compensatory base substitutions, we found that two elements interfere with the formation of SL1-dependent tight dimers. The cores of these elements are located at nucleotides 189−196 and 543−550. Our results suggest that base pairing between these sequences prevents the formation of SL1-dependent tight dimers, probably by sequestering SL1 in a stable intramolecular arrangement. Moreover, we found that nucleotides downstream of SL1 decreased the rate of tight dimerization. Interestingly, dimerization at 37 °C in the presence of nucleocapsid protein increased the yield of SL1-mediated tight dimerization *in vitro*, even in the presence of the two interfering elements, suggesting a relationship between the nucleocapsid protein and activation of the SL1 dimerization signal *in vivo*.

Retroviruses encapsidate two copies of genomic single-stranded RNA in their infectious particles. Electron microscopy studies of the organization of genomic RNA isolated from retroviral particles revealed that the two strands are associated through a region located close to the 5′-end, called the dimer linkage structure (DLS)[1] (*1*; for HIV-1, see ref *2*). Upon budding, retroviral particles undergo a maturation event that involves changes in the stability of the genomic RNA dimer (*3*, *4*) which may be reminiscent of the loose−tight dimer interconversion observed *in vitro* (described below).

Several model systems have been developed to study dimerization of the DLS. RNA fragments corresponding to the 5′-end of the genomic RNA have been shown to dimerize *in vitro* in the absence of any viral or cellular protein (in the case of HIV-1, see ref *5*). Further analysis identified a short RNA sequence that promotes dimerization of HIV-1 transcripts *in vitro* and was named the dimerization initiation site (DIS) (*6*, *7*) or stem−loop 1 [SL1 (*8*)]. Studies of the dimerization properties of HIV-2 leader RNA yielded results different from those obtained with similar HIV-1 fragments. First, an HIV-2 RNA fragment encompassing the complete leader region of the genomic RNA and the first several codons of the Gag protein (Figure 1A) was found to use the 5′-end of the primer-binding site (PBS), and not the expected SL1, as a dimer-inducing element at physiological temperature (37 °C) (*9*). Its properties were characteristic of a so-called loose dimer (*10*, *11*). In general, loose dimers can be observed on a native gel in Tris-borate magnesium (TBM) buffer at 4 °C but are absent when assayed either on a semidenaturing gel in Tris-borate EDTA (TBE) buffer or on a TBM gel at 24 °C, presumably because the dimers dissociate under these electrophoresis conditions (*12*). Loose dimers of HIV-1 RNA are thought to be associated via an intermolecular kissing loop interaction (*10*, *11*, *13*−*15*).

A second way in which HIV-1 and HIV-2 RNAs behave differently is that the HIV-2 leader RNA fragment was unable to form tight dimers (*16*, *17*), contrary to HIV-1 RNA (*10*, *11*, *18*). These exceptionally stable dimers could withstand semidenaturing electrophoresis in TBE buffer at 24 °C. In HIV-2, only a shorter RNA (residues 1−444), in which SL1 is located at the extreme 3′-end, was able to form a SL1-dependent tight dimer upon incubation at high temperatures (*16*, *17*, *19*). Thus, the use of the SL1 dimer-inducing element depends on the size of the RNA fragment,

† This research was supported by National Institutes of Health Grant AI45388 to J.S.L.

* To whom correspondence should be addressed. Telephone: (406) 243-6393. Fax: (406) 243-4304. E-mail: lodmell@selway.umt.edu.

[1] Abbreviations: HIV-1 and -2, human immunodeficiency virus types 1 and 2, respectively; SL1, stem−loop 1; PBS, primer binding site; DIS, dimerization initiation site; DLS, dimer linkage structure; TBE, Tris-borate EDTA buffer; TBM, Tris-borate magnesium buffer; NCp7, nucleocapsid protein.

10.1021/bi0271190 CCC: $25.00
Published on Web 02/11/2003

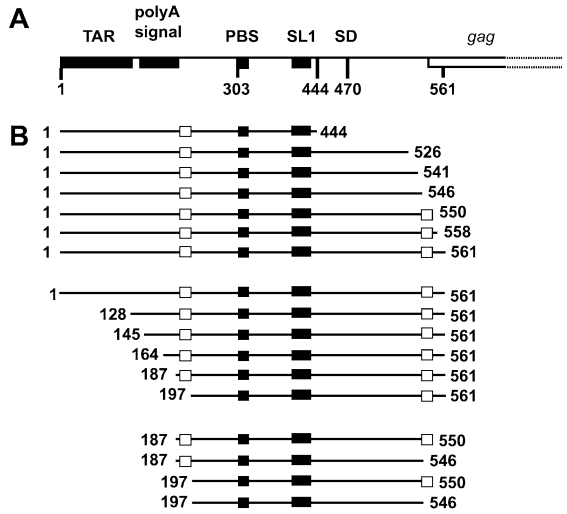

FIGURE 1: 5′-leader region of HIV-2 *ROD* genomic RNA. (A) The landmark sequences with known functions are shown as boxes. TAR, polyA signal, PBS, SL1, SD, and *gag* represent the transactivation region, the poly(A) signal domain, the primer-binding site, the stem−loop 1 structure, the major splice donor site, and the 5′-end of the Gag protein coding region, respectively. (B) RNAs used in this study. The filled boxes represent the two dimer-inducing elements, namely, the 5′-end of the PBS and SL1. The empty boxes represent the cores of the two dimer-interfering elements characterized in this study, residues 189−196 and 543−550. The numbers to the left and right indicate the 5′- and 3′-termini of the various RNAs used here, respectively.

as large RNAs [up to 950 nucleotides long (*17*)] are unable to form tight dimers *in vitro* despite the presence of the SL1 element in their sequences. This observation suggests the presence of elements which interfere with tight dimerization, especially downstream of SL1 and the major splice donor site, as was previously proposed (*17*).

In this study, we analyzed the influence of sequences upstream and downstream of the major splice donor site on the formation of HIV-2 leader RNA dimers *in vitro* using a variety of RNA constructs and dimerization and electrophoresis protocols. We tested the properties of 1−444 and 1−561 model RNAs formed at 37 or 55 °C to assay for the formation of loose or tight dimers and to determine the relative use of the PBS region and SL1 dimer-inducing elements. Although both RNAs could form PBS-dependent loose dimers, the 1−561 RNA was unable to form SL1-dependent tight dimers upon incubation at 55 °C, unlike the 1−444 RNA. Using RNAs truncated at their 5′- or 3′-ends, we found that two elements prevent the formation of SL1-dependent tight dimers of the HIV-2 leader RNA. The cores of these interfering elements were localized between nucleotides 189−196 and 543−550, and verified using site-directed mutagenesis and compensatory mutations. Our dimerization results indicate that base pairing between these sequences prevents the use of SL1 in the formation of a tight dimer, probably by sequestering SL1 in a stable intramolecular base pairing arrangement. Furthermore, sequences between nucleotides 444 and 546 influenced the *rate* of tight dimerization. We also tested the influence of the nucleocapsid protein on the formation of a tight dimer with 1−444 and 1−561 RNAs and observed that, as in the HIV-1 system, the yield of SL1-mediated tight dimerization increased in the presence of nucleocapsid protein, even with the large HIV-2 leader RNA fragments that were unable to form tight dimers without protein. Since the SL1 structure is very close to the core encapsidation signal of HIV-2 RNA (*20*) and one of the dimer-interfering elements encompasses the *gag* initiation codon, our results suggest a model of how the processes of translation, dimerization, and encapsidation of HIV-2 RNA and proteins could be interdependent *in vivo*.

MATERIALS AND METHODS

Template Construction for in Vitro Transcription. A sense primer containing a *Bam*HI site and the promoter for the T7 RNA polymerase and an antisense primer containing an *Eco*RI site (Table 1) were used to amplify the first 381, 444, 526, 541, 546, 550, 558, or 561 nucleotides of the HIV-2 genomic RNA sequence, *ROD* isolate. The HIV-2 *ROD* DNA template (modified plasmid pROD10) was provided by the EU Programme EVA/MRC Centralised Facility for AIDS Reagents, NIBSC, UK (Grants QLK2-CT-1999-00609 and GP828102). The numbering is based on the genomic RNA sequence. The 5′-truncated fragments were made using a sense primer containing a *Bam*HI site, the promoter for the T7 RNA polymerase, and starting at different positions of the genomic RNA (nucleotide 128, 145, 164, 187, or 197), and an antisense primer containing an *Eco*RI site and a HIV-2 sequence ending at nucleotide 561. The plasmid containing the first 290 nucleotides of HIV-1 *Lai* genomic RNA was constructed using a similar strategy. The HIV-1 p83-2 template plasmid was obtained from R. Desrosiers through the AIDS Research and Reference Reagent Program, Division of AIDS, National Institute of Allergy and Infectious Diseases (NIAID), National Institutes of Health (NIH) (Bethesda, MD) (*21*). The digested PCR (polymerase chain reaction) products were cloned in the *Bam*HI and *Eco*RI sites of the pUC18 plasmid. The base substitutions in the upstream and downstream elements were made using mutagenic primers sBAMT7GEE and asECOCEE to amplify the construct of nucleotides 187−550. The construct of nucleotides 1−444 harboring a deleted loop in SL1 was described previously.

RNA Synthesis and Purification. The different plasmids were linearized with *Eco*RI prior to *in vitro* transcription. RNAs were synthesized by *in vitro* transcription of the *Eco*RI-digested plasmids with the AmpliScribe T7 transcription kit (Epicentre). After transcription, the DNA was digested with the supplied RNase-free DNase, and the RNA was purified by ammonium acetate precipitation followed by size exclusion chromatography (Bio-Gel P-4, Bio-Rad).

In Vitro Dimerization of HIV-2 RNA. Five to seven picomoles of RNA was denatured in 8 μL of water for 2 min at 90 °C and quench-cooled on ice for 2 min. After the addition of 2 μL of monomer buffer [50 mM Tris-HCl (pH 7.5) at 37 °C, 40 mM KCl, and 0.1 mM $MgCl_2$ (final concentrations)] or dimer buffer [50 mM Tris-HCl (pH 7.5) at 37 °C, 300 mM KCl, and 5 mM $MgCl_2$ (final concentrations)], dimerization was allowed to proceed for 15−60 min at 37 or 55 °C. We compared 37 to 55 °C since the incubation of the 1−444 RNA at 55 °C allows a maximal yield of TBE-resistant SL1-dependent dimers (*17*). The samples were then cooled on ice to stabilize dimers formed during incubation and loaded on a 0.8% agarose gel with 2 μL of glycerol loading dye [6×: 40% glycerol, 44 mM Tris-borate (pH 8.3), and 0.25% bromophenol blue]. Electro-

Table 1: Oligonucleotides Used in This Study[a]

sBAMT7LAI	TAG GAT CCT AAT ACG ACT CAC TAT AGG TCT CTC TGG TTA GAC C
sBAMT7R	TAG GAT CCT AAT ACG ACT CAC TAT AGG TCG CTC TGC GGA GAG
sBAMT7128	TAG GAT CCT AAT ACG ACT CAC TAT AGG CTT GCT TGC TTA AAA ACC TC
sBAMT7145	TAG GAT CCT AAT ACG ACT CAC TAT AGG CCT CTT AAT AAA GCT GCC AG
sBAMT7164	TAG GAT CCT AAT ACG ACT CAC TAT AGG TTA GAA GCA AGT TAA GTG
sBAMT7187	TAG GAT CCT AAT ACG ACT CAC TAT AGG CTC CCA TCT CTC CTA GTC
sBAMT7197	TAG GAT CCT AAT ACG ACT CAC TAT AGG TCC TAG TCG CCG CC
sBAMT7GEE	ATG GAT CCT AAT ACG ACT CAC TAT AGG CTG GGT AGA GTC CTA GTC GCC GCC TGG
asECOCEE	TTG AAT TCG GGT AGA GCC ACA ATC TTC TAC CTG TC
asECOLAI	AAG AAT TCC AGT CGC CGC CCC
asECO444	AAG AAT TCG CTC CAC ACG CTG CCT TTG
asECO526	AAG AAT TCG TCT AAA GGT AGG ATA G
asECO541	AAG AAT TCA CAA TCT TCT ACC TG
asECO546	AAG AAT TCT CCC ACA ATC TTC TAC C
asECO550	AAG AAT TCC CAT CTC CCA CAA TC
asECO558	AAG AAT TCT CGC GCC CAT CTC CC
asECO561	AAG AAT TCA GTT TCT CGC GCC CAT CTC CC

[a] The 5′−3′ sequence is indicated from left to right.

phoresis was carried out for 2 h at 4 °C and 5 V/cm in 44 mM Tris-borate (pH 8.3) and 0.1 mM $MgCl_2$ (TBM) or at room temperature (24 °C) in 44 mM Tris-borate (pH 8.3) and 1 mM EDTA (TBE). After electrophoresis, the ethidium bromide-stained gel was scanned on a Fluorescent Image Analyzer FLA-3000 (Fujifilm).

Kinetics of Tight Dimer Formation. One hundred picomoles of RNA was denatured in 160 μL of water for 2 min at 90 °C and quench-cooled on ice for 2 min. After the addition of 2 μL of dimer buffer [50 mM Tris-HCl (pH 7.5) at 37 °C, 40 mM NaCl, and 5 mM $MgCl_2$ (final concentrations)] under the lid of 20 tubes, 8 μL of denatured RNA was aliquoted to each tube. The dimerization was then initiated by a 5 s spin in a benchtop centrifuge and immediate loading of the tubes in a heating block at 50, 55, or 60 °C. Dimerization was allowed to proceed for 2−60 min or longer. At each time point, a tube containing 10 μL of reaction mixture was removed from the heating block, mixed with 2 μL of glycerol loading dye 6x, and loaded on a 0.8% agarose TBE gel. Electrophoresis was carried out at room temperature (24 °C) and 3 V/cm. After electrophoresis, the ethidium bromide-stained gel was scanned on a Fluorescent Image Analyzer FLA-3000 (Fujifilm). Quantification of the extent of dimerization was done using Fujifilm Image Gauge version 3.3. The data were fitted using a second-order conformation model (*23*):

$$1/M_t = 1/M_0 + 2k_{dim}t$$

where M_t is the concentration of the monomer at time t, M_0 is the initial concentration of the dimerization-competent monomer, and k_{dim} is the second-order rate constant of dimerization (μM^{-1} min^{-1}).

NCp7-Mediated Tight Dimerization Assay. The HIV-1 nucleocapsid protein NCp7 was kindly provided by J. Marino. This protein was expressed in *Escherichia coli* and purified by chromatography (for further details, see ref *24*). We based our NCp7-mediated dimerization assay on the protocol described by Muriaux *et al.* for an HIV-1 *Lai* isolate RNA fragment and nucleocapsid protein (*25*). Five picomoles of RNA was denatured in water for 2 min at 90 °C and quench-cooled on ice for 2 min. After the addition of monomer or dimer buffer, dimerization was allowed to proceed for 30 min at 37 or 55 °C. Tubes containing 125 pmol of NCp7 in monomer buffer were incubated at 37 °C for 30 min. The concentration of NCp7 (around one protein per 20 nucleotides) allows complete tight dimerization of the homologous HIV-1 RNA (*25*). Since NCp7 binding to the RNA changes the electrophoretic properties of the RNA and prevents the analysis of monomer and dimer levels, an SDS/phenol extraction step is necessary. Tubes containing the NCp7 and control tubes incubated at 37 or 55 °C without NCp7 were incubated for 2 min at 24 °C with 0.2% SDS and then extracted with phenol-saturated with 0.2% SDS and monomer buffer 1x. All samples were then loaded on a 0.8% agarose TBE gel. Electrophoresis was carried out at room temperature (24 °C) and 5 V/cm. After electrophoresis, the ethidium bromide-stained gel was scanned on a Fluorescent Image Analyzer FLA-3000 (Fujifilm).

RESULTS

The Complete HIV-2 Leader RNA Cannot Form Tight Dimers in Vitro. We compared the effect of different incubation temperatures (37 or 55 °C) and different electrophoretic conditions on the dimerization of 1−444 and 1−561 RNA fragments. Both RNA constructs contain the PBS and SL1 sequences, with SL1 at the extreme 3′-end of the 1−444 fragment (Figure 1). The incubation temperature of 55 °C was chosen because it allows efficient formation of tight dimers *in vitro* for HIV-1 RNA (*11*) and HIV-2 1−444 RNA (*17*). Both RNAs were able to dimerize when assayed on a TBM gel at 4 °C (Figure 2A). We previously showed that both RNAs use the 5′-end of the PBS as a dimer-inducing element when incubated at 37 °C (Figure 1A and ref *17*). However, only the 1−444 fragment dimerized when the RNAs were loaded on a TBE gel at 24 °C (Figure 2B). The 1−561 RNA did not dimerize significantly under these electrophoresis conditions after incubation at 37 or 55 °C (Figure 2B, lanes 9 and 10). The formation of small amounts of 1−561 TBE-resistant dimers required the 55 °C incubation step in monomer or dimer buffer (Figure 2B, lanes 8 and 10).

Thus, an RNA that encompasses the complete leader region of HIV-2 was not able to form a tight dimer *in vitro*, even though it contains two distinct dimer-inducing elements. Since we and others demonstrated that the tight dimer of 1−444 RNA occurs through the stem−loop 1 sequence (SL1) (*17, 19*), this result suggested that, in the 1−561 RNA, all

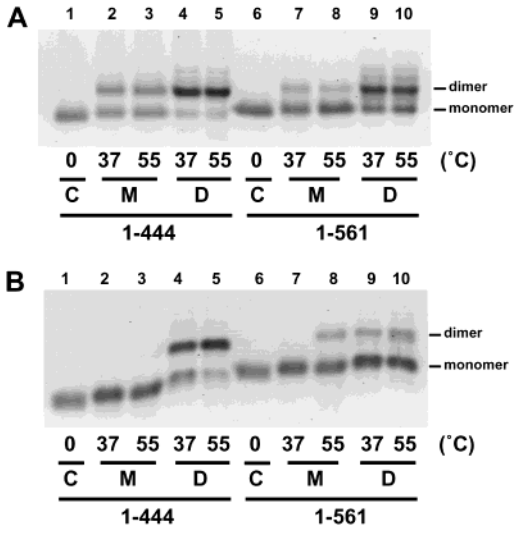

FIGURE 2: Differential dimerization properties of 1−444 and 1−561 RNAs. 1−444 and 1−561 RNAs were assayed for dimerization with monomer (M) or dimer (D) buffer at 37 or 55 °C. After incubation for 30 min, duplicates were subjected to electrophoresis on agarose gels. (A) Electrophoresis was carried out in TBM buffer at 4 °C. (B) Electrophoresis was carried out in TBE buffer at 24 °C. The two different electrophoresis conditions allow comparison of the stabilities of the dimers. Loose and tight dimers are observed on TBM gels, but only tight dimers withstand the TBE electrophoresis.

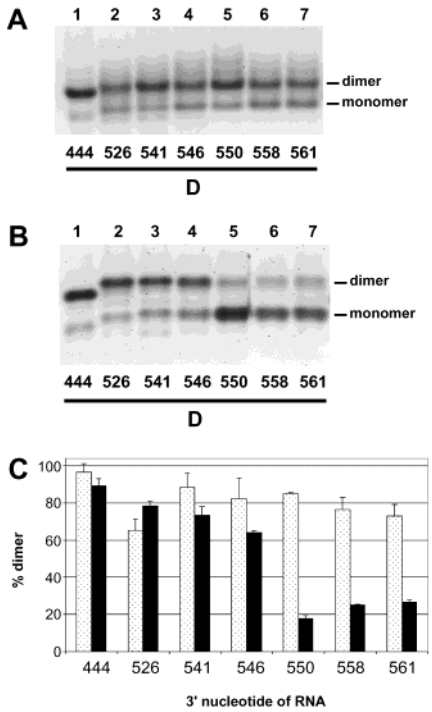

FIGURE 3: Dimerization of RNAs harboring 3′-truncations. RNAs were incubated in high-potassium and high-magnesium dimer buffer, and duplicates were subjected to electrophoresis on agarose gels. The number below each lane indicates the final 3′-nucleotide. (A) Electrophoresis was carried out in TBM buffer at 4 °C. (B) Electrophoresis was carried out in TBE buffer at 24 °C. (C) Percent dimerization for each RNA when assayed on a TBM gel at 4 °C (stippled bars) or a TBE gel at 24 °C (filled bars). The *y*-axis error bars represent the standard deviation of replicate experiments.

or part of the SL1 sequence may be involved in an intramolecular interaction that prevents formation of an extended intermolecular SL1−SL1 interaction (i.e., a tight dimer). More specifically, these results indicate that the formation of this intramolecular interaction depends on a structural element located between nucleotides 444 and 561.

Influence of the 3′-Terminal Sequence on Tight Dimer Formation. To further define the element(s) that prevents the formation of the SL1-mediated 1−561 RNA tight dimer, we assayed dimerization of RNA fragments of different lengths. An unconstrained M-fold folding of the 1−561 RNA indicated a long-range interaction of sequences located between the poly(A) signal and PBS domains, and sequences located near the 3′-end of the 1−561 RNA (Figures 1 and 7; *26*, *27*). We therefore synthesized HIV-2 RNAs comprising nucleotides 1−526, 1−541, 1−546, 1−550, and 1−558 to test the effects of these sequences (Figure 1B). After incubation in high-potassium and high-magnesium dimer buffer at 37 or 55 °C, the RNAs were loaded either on a TBM gel at 4 °C (Figure 3A) or on a TBE gel at 24 °C (Figure 3B), respectively. All RNAs formed dimers at 37 °C when observed on a TBM gel at 4 °C. Using antisense oligonucleotides, we checked that the sequence engaged in the 37 °C dimerization of these RNAs involves the 5′-end of the PBS (J.-M. Lanchy and J. S. Lodmell, data not shown). When the 55 °C-incubated RNAs were assayed for tight dimerization on a TBE gel at 24 °C, RNAs longer than 550 nucleotides formed very small amounts of dimer compared to RNAs smaller than 546 nucleotides (Figure 3B, compare lanes 1−4 to lanes 5−7). From this result, we conclude that one interfering element is located upstream of nucleotide 550 and that the very different behaviors of 1−546 and 1−550 RNAs indicated that the core of this element may be located between nucleotides 546 and 550.

Influence of 5′-Terminal Truncations on the Putative Long-Range Interaction. Computer-assisted folding of the model 1−561 RNA (*26*, *27*) almost always suggested a long-range interaction between nucleotides 189−196 and 543−550 (Figures 1 and 7). Therefore, we hypothesized that truncations at the 5′-end of RNAs terminating at nucleotide 561 should promote tight dimerization if the deletion included nucleotides involved in the putative long-range base pairing. We constructed and tested different RNAs for their ability to dimerize. The 5′-ends of these truncated RNAs were at positions 128, 145, 164, 187, and 197, relative to the full-length wild-type RNA (Figure 1B). As shown in Figure 4A, these RNAs could form dimers when incubated at 37 °C in a high-potassium and high-magnesium buffer and loaded onto a TBM gel run at 4 °C. Using antisense oligonucleotides directed against either the PBS or the SL1 sequence, we determined that the 5′-end of the PBS was responsible for the dimerization under these conditions (data not shown). However, when these RNAs were loaded onto a TBE gel at 24 °C, only the 197−561 RNA presented a high yield of dimer (very close to 100%; Figure 4B, lane 6). Comparison of lanes 1 and 2 to lanes 3−5 also indicated that a low level of *in vitro* dimerization/multimerization might be mediated by the TAR and poly(A) signal regions.

Thus, the 5′-truncation of the upstream sequence had the same effect on dimerization as the truncation of the putative 3′-partner sequence, which strongly suggests that the two sequences are involved in a long-range interaction.

Effects of Simultaneous 5′- and 3′-Truncations on Dimerization. To ensure that the effect on dimerization of the 5′-

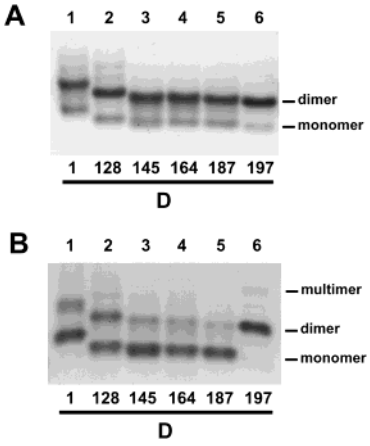

FIGURE 4: Dimerization of RNAs harboring 5′-truncations. The number under each lane indicates the 5′-terminus for each RNA; the 3′-terminus of each RNA was position 561. RNAs were incubated in high-potassium and high-magnesium dimer buffer, and duplicates were subjected to agarose electrophoresis. (A) Electrophoresis was carried out in TBM buffer at 4 °C. (B) Electrophoresis was carried out in TBE buffer at 24 °C.

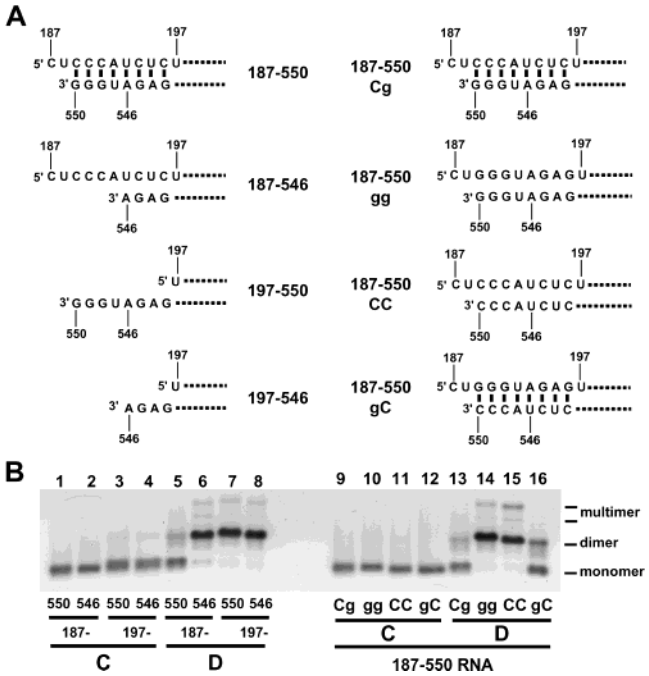

FIGURE 5: Dimerization of RNAs harboring simultaneous 5′- and 3′-deletions or mutations in the sequences involved in the long-range interaction. (A) Schematic of the sequences involved in the long-range interaction for all of the RNAs used in panel B. In the left column, the 5′- and 3′-truncations used for lanes 1−8 of panel B are shown. The right column shows the strategy employed to disrupt and restore base pairing between the upstream and downstream long-range interaction elements. 187−550 Cg shows the wild-type interaction. In the 187−550 gg mutant, the wild-type upstream element has been replaced with an inverted copy of the downstream element, which destroys base pairing. In the 187−550 CC mutant, the downstream element has been replaced with an inverted copy of the upstream element, again destroying base pairing between the two elements. In the 187−550 gC compensatory mutant, the upstream and downstream inverted elements were swapped, effectively restoring potential base pairing between the elements. (B) Results of dimerization experiments conducted with the RNAs depicted in panel A. Lanes 1−4 and 9−12 show denatured monomeric RNA. On the left side of the gel, lanes 5−8 demonstrate that only 187−550 RNA (lane 5), containing both the upstream and downstream elements, is not capable of efficient tight dimerization. The combinations of truncated RNAs that lack either or both long-range interaction elements dimerize very efficiently (lanes 6−8). On the right side of the gel, the wild-type and 187−550 gC RNAs, which are capable of forming base pairs between the upstream and downstream elements, do not dimerize efficiently (lanes 13 and 16), while the 187−550 gg and CC mutants dimerize completely (lanes 14 and 15).

and 3′-truncations could be attributed to the loss of the long-range interaction between the upstream and downstream RNA elements, we tested the dimerization properties of RNAs harboring truncations at both the 5′- and 3′-ends (Figure 5). In particular, we compared the dimerization of RNAs 187−550, 187−546, 197−550, and 197−546. As predicted by the truncation experiments described above, the only RNA that did not form TBE stable dimers was the 187−550 RNA which contained both elements involved in the long-range interaction. Truncations of either the upstream or downstream element or deletion of both elements at the same time resulted in RNAs that efficiently formed TBE stable dimers, strongly implicating that the loss of the long-range interaction, and not an independent effect of the truncations, was responsible for allowing formation of tight dimers.

Site-Directed Mutagenesis and Compensatory Mutations Confirm the Long-Range Interaction. The truncation analysis suggested that base pairing between the upstream and downstream elements of the long-range interaction inhibited the capacity to form tight dimers. To explicitly test this, we introduced mutations into both sequences, either independently or together (Figure 5). The results clearly demonstrated that interfering with base pairing between the upstream and downstream elements allowed formation of tight dimers, while restoration of base pairing by swapping the 5′- and 3′-sequences resulted in RNAs that were compromised in their ability to form tight dimers.

Kinetic Influence of the 3′-Terminal Sequence. Even though all RNAs smaller than 546 nucleotides were able to form a high level of tight dimer after incubation for 1 h at 55 °C, the quantification of two to three independent experiments indicated that their behavior was different. The yield of tight dimerization decreased when more sequence was present at the 3′-end of the RNA beyond position 444 (Figure 3B, lanes 1−4, and Figure 3C). We therefore investigated whether the presence of nucleotides downstream of SL1 influenced the rate of tight dimerization.

We performed kinetic analysis of tight dimerization at different incubation temperatures (50, 55, or 60 °C) for 1−444, 1−526, 1−541, and 1−546 RNAs, assayed on a TBE gel at 24 °C. To aid in the direct comparison of the results of this experiment with results of a previous study (*16*), we used a low-sodium and high-magnesium dimerization buffer. Results obtained using a high-potassium and high-magnesium dimerization buffer were very similar (data not shown). A typical experiment is shown in Figure 6A (1−526 RNA at 55 °C), and in Figure 6B, the dimerization kinetics at 55 °C of 1−444, 1−526, 1−541, and 1−546 RNAs are represented. To determine the dimerization rate constant, the data were fitted using a second-order reaction model (see Materials and Methods). At 55 °C, the dimerization rate of the 1−444 RNA was 2−3-fold faster than those of the other RNAs (Figure 6B,C). Analysis of the dimerization rates at different temperatures revealed two

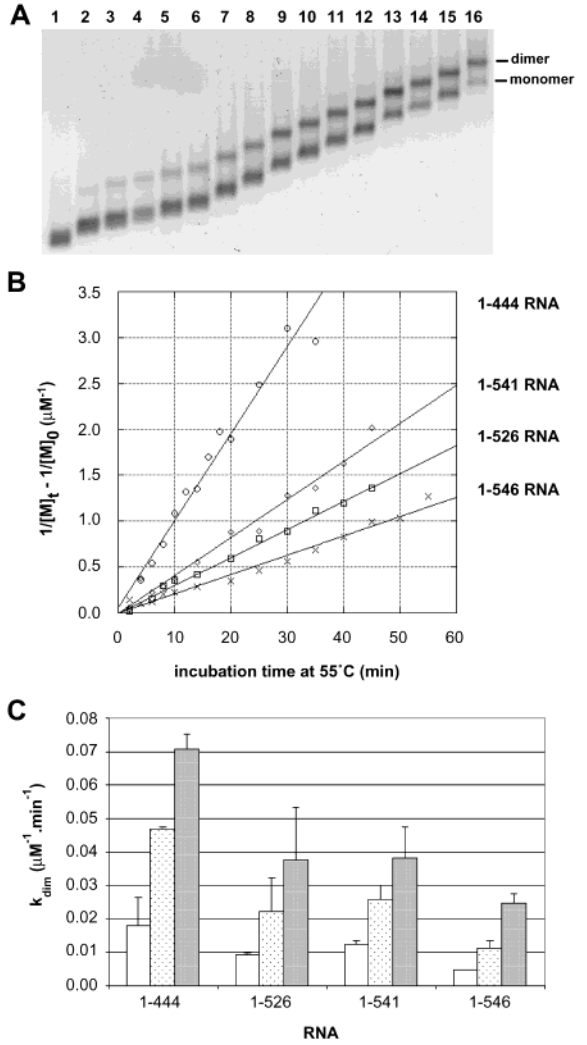

FIGURE 6: Kinetics of tight dimerization of 1−444, 1−526, 1−541, and 1−546 RNAs at different temperatures. (A) The time-dependent yield of dimerization of 1−526 RNA at 55 °C was monitored on a TBE agarose gel at 24 °C. Lanes 1−16 represent incubation times of 0, 2, 4, 6, 8, 10, 15, 20, 25, 30, 35, 40, 45, 50, 55, and 60 min, respectively. (B) Plots of the kinetic data for 1−444, 1−526, 1−541, and 1−546 RNAs. $[M]_t$ is the concentration of monomer at time t, and $[M]_0$ is the initial concentration of the dimerization-competent monomer. (C) Kinetic constants, k_{dim}, were obtained by fitting the data to a second-order reaction model (*23*). The resulting dimerization rates are represented for the different RNAs and incubation temperatures. Empty, stippled, and filled bars correspond to the 50, 55, and 60 °C incubation temperatures, respectively. The *y*-axis error bars represent the standard deviation of replicate experiments.

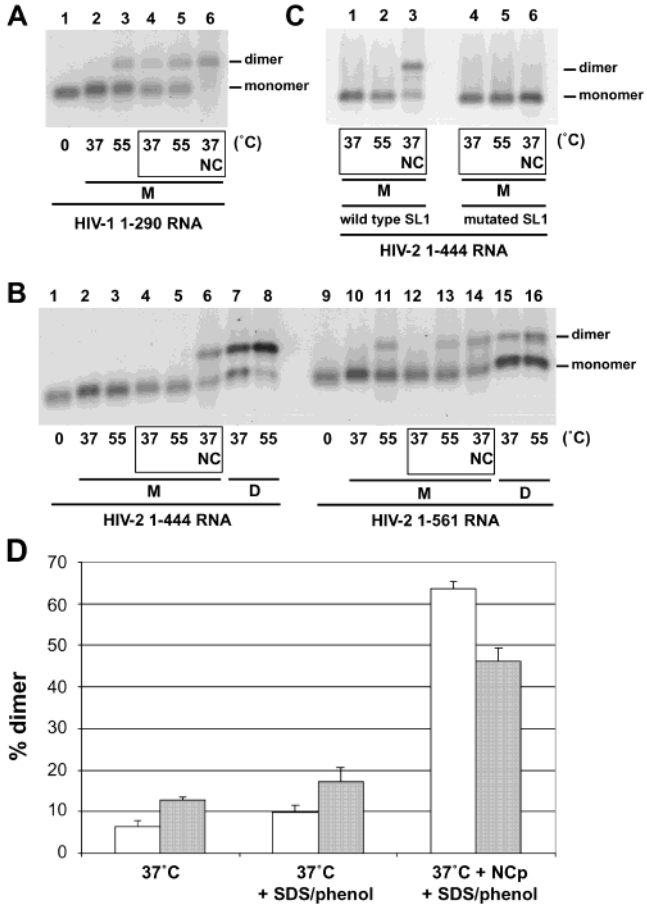

FIGURE 7: Influence of the nucleocapsid protein on the dimerization of 1−444 and 1−561 RNAs. (A) HIV-1 *Lai* 1−290 RNA was incubated for 30 min at 37 or 55 °C with or without HIV-1 nucleocapsid protein NCp7 in monomer buffer [50 mM Tris-HCl (pH 7.5), 40 mM potassium, and 0.1 mM magnesium]. After SDS/phenol extraction, the samples were loaded on a TBE gel at 24 °C. (B) HIV-2 *ROD* 1−444 (left) and 1−561 (right) RNAs were incubated as described for panel A. Two supplementary lanes showed incubation of the RNAs in dimer buffer (high-potassium and high-magnesium) without NCp7 at 37 (lanes 7 and 15) or 55 °C (lanes 8 and 16). SDS/phenol-extracted samples are boxed. (C) The 1−444 wild type (lanes 1−3) or 1−444 with the GUAC sequence deleted from the apical SL1 loop (lanes 4−6) was dimerized at 37 °C with or without NCp, or at 55 °C without NCp, as indicated. The RNAs lacking an intact SL1 were incapable of forming a TBE stable tight dimer. (D) Plot of dimerization yield as a function of SDS/phenol extraction and presence of NCp7 at 37 °C for the 1−444 (empty bars) and 1−561 (filled bars) RNAs. The *y*-axis error bars represent the standard deviation of two experiments.

interesting results. First, the 1−444 RNA dimerized more rapidly at every temperature that was tested (50, 55, and 60 °C, Figure 6C) than any other RNA. Second, the dimerization rates of all RNAs increased with temperature, approximately doubling with each 5 °C increase in temperature (Figure 6C).

Thus, the 3′-terminal location of the SL1 structure in the 1−444 RNA corresponded to a positive kinetic effect on the rate of tight dimer formation. The presence of nucleotides downstream of the SL1 structure negatively affected the ability of large RNAs to form tight dimers *in vitro*, probably by forcing or sequestering all or part of SL1 into a more stable intramolecular structure. This inhibition of the use of SL1 for tight dimerization was maximal when the RNA was 550 nucleotides or longer.

Effect of Nucleocapsid Protein on Dimerization. Since the genomic RNA interacts with the Gag precursor polyprotein predominantly through its nucleocapsid domain during encapsidation and later steps, we wished to examine the effects of nucleocapsid protein (NCp7) on the dimerization of various RNA constructs. We used HIV-1 NCp7 protein which was kindly provided by J. Marino and purified as described previously (*24*). First, we verified that the incubation at 37 °C of HIV-1 1−290 RNA with NCp7 yielded the same amount of TBE-resistant dimer as incubation at 55 °C without NCp7 (Figure 7A and ref *25*). Second, 1−444 and 1−561 HIV-2 RNAs were incubated with or without NCp7. Since there is an obligatory SDS/phenol extraction for removal of NCp7 from the RNA before loading on the gel, we also included controls to show that this extraction step

did not influence RNA dimerization (Figure 7B, compare lanes 2, 3, 10, and 11 to lanes 4, 5, 12, and 13, respectively). There was a low of yield of the dimer of 1−561 RNA with an incubation temperature of 55 °C. We showed previously that these dimers were not sensitive to the antisense oligonucleotides directed against PBS or SL1 dimer-inducing elements (*17*), and they appear from results in Figure 4B to be TAR−TAR dimers (compare lanes 1 and 2 to lanes 3−5).

When the 1−444 RNA was incubated with NCp7 at 37 °C, and SDS/phenol extracted, the level of tight dimer was almost as high as when this RNA was incubated in dimer buffer at 55 °C (Figure 7B, compare lane 6 to lane 8, and Figure 7C). The level of 1−561 tight dimer reached 45% in the presence of NCp7 (Figure 7B, lane 13, and Figure 7C), which is 3-fold higher than for a protein-free dimerization at 37 °C (Figure 7B, lane 12) or 2-fold higher than for a 55 °C dimerization (Figure 7B, lane 16). Thus, incubation of the 1−561 RNA with the mature form of the nucleocapsid protein promotes the use of SL1 and allows the formation of a stable tight dimer, although the presence of sequence downstream of the SL1 structure may reduce the yield *in vitro*.

To verify that NCp catalyzed the formation of tight dimers through SL1 and not through another point of contact, we repeated the dimerization assay using NCp with wild-type 1−444 RNA and 1−444 RNA harboring a deletion in the loop of SL1 (*22*). The results of this experiment are presented in Figure 7C. Nucleocapsid protein efficiently converted wild-type 1−444 RNA to tight dimers at 37 °C (lanes 1−3), but failed to convert the SL1 mutant 1−444 RNA to tight dimers (lanes 4−6). This result strongly suggests that the principal tight dimerization site is at SL1.

Computer-Assisted Folding of the 1−561 HIV-2 RNA. The secondary structure model of the 1−561 RNA in Figure 8 shows a possible secondary structure arrangement that maintains the long-range interaction and simultaneously makes the SL1 sequence unavailable for intermolecular base pairing. The model was constructed using M-fold 3.0 software with two local constraints (*26*, *27*). First, nucleotides 34−39 were kept single-stranded so that the TAR domain would adopt the empirically determined bifurcated conformation and not the thermodynamically more stable conformation (*28*, *29*). Second, preliminary results of RNA chemical probing experiments indicated that nucleotides A423 and A426 located in the loop of SL1 are not accessible to chemical probes specific for single-stranded nucleotides when the 1−561 RNA is incubated at 55 °C, but are susceptible to chemical modification when mutations are present in the RNA that allow SL1-mediated dimerization (J. D. Ivanovitch and J. S. Lodmell, data not shown). Thus, for this model, we constrained nucleotides A423 and A426 to be double-stranded, although in a strict sense the loss of reactivity could also be due to base stacking. The resulting most stable structure is shown in Figure 8. Although this model was constructed using additional constraints based on structural data for the TAR and the 423+426 regions, the long-range interaction we propose is also found when the 1−561 RNA is folded without constraint. It is notable that other nearly isoenergetic M-fold structures depict SL1 in its "classic" stem−loop structure, suggesting that this region may be able to change conformations without a large thermodynamic cost.

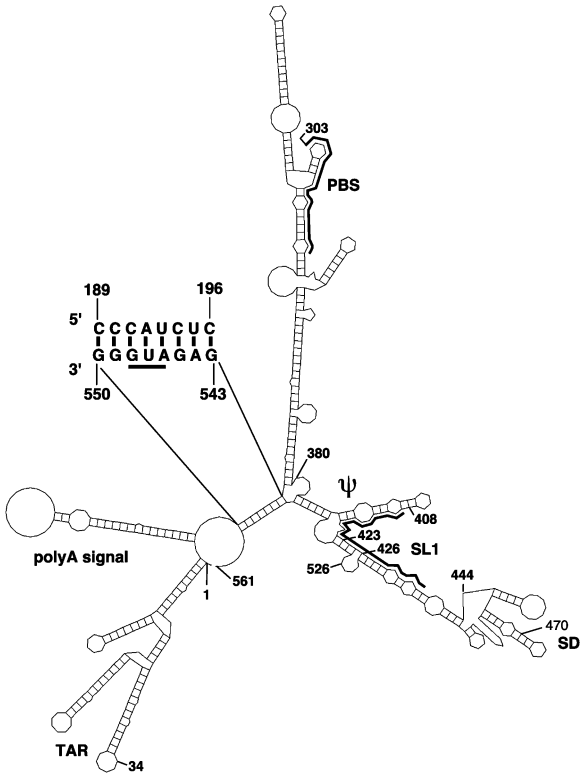

FIGURE 8: Secondary structure model of the HIV-2 *ROD* leader RNA. The model was generated using M-fold (*26*, *27*) and represents the most stable secondary structure returned for the 1−561 RNA that also agrees with the biochemical analysis (see the Results). The proposed long-range base pairing between nucleotides 189−196 and 543−550 is indicated at the left of the figure. The *gag* initiation codon is indicated by the solid horizontal bar below the sequence. ψ represents the core encapsidation signal of HIV-2 genomic RNA (nucleotides 380−408) defined by deletion mutagenesis (*20*). Thick lines indicate the PBS and the entire SL1 sequence [nucleotides 409−439 (*29*)].

DISCUSSION

In this study, we analyzed the *in vitro* dimerization properties of HIV-2 leader RNA fragments, focusing especially on the use of two previously described dimer-inducing elements: the 5′-end of the primer-binding site (PBS) and the stem−loop 1 structure (SL1) (Figure 1) (*9*, *17*, *19*). We showed that an HIV-2 leader RNA could use the 5′-end of the PBS as a loose dimer-inducing element at physiological (37 °C) or high (55 °C) incubation temperatures. This dimerization is a salt-dependent process: the optimal dimerization buffer contains 300 mM potassium and 5 mM magnesium, while our monomer buffer contains 40 mM potassium and 0.1 mM magnesium. It is interesting to note that the concentration of intracellular potassium was found to be higher in HIV-1-infected T cells than in noninfected cells [200−400 and 100−130 mM, respectively (*30*)]. This difference may positively influence HIV-2 RNA dimerization *in vivo*. The PBS−PBS interaction in 1−444 and 1−561 RNA dimers is characteristic of a loose dimer, as described for the HIV-1 *Lai* SL1−SL1 interaction (*10*, *11*), and may indicate the involvement of a magnesium-dependent tertiary structure element(s). A similar feature has been described for HIV-1 *Mal* RNA dimerization (*31*, *32*).

In a previous paper, we showed that the nature and position of the 3′-end of the construct and, to a lesser degree the

dimerization protocol, influenced the use of the SL1 dimer-inducing element in the HIV-2 leader sequence (*17*). The structure and the location of this element are homologous to those of HIV-1 SL1, which is the element that mediates dimerization of HIV-1 RNA fragments *in vitro* (*5*−*7*, *13*, *14*, *33*, *34*). However the HIV-2 SL1 sequence does not mediate the formation of loose dimers *in vitro*, either as an isolated structure (*9*) or as a structural element in the 1−561 RNA (*17*). In contrast, the 1−444 RNA was uniquely able to form SL1-dependent tight dimers upon incubation at high temperatures (*17*, *19*). These tight dimers are defined by their resistance to dissociation during electrophoresis at room temperature and in the presence of EDTA. The tight dimer behavior of small HIV-1 or HIV-2 RNAs is thought to be caused by an extended base pairing arrangement of SL1 (first proposed in refs *6*, *33*, and *34* and further analyzed in refs *10*, *11*, and *15*). The 1−444 RNA is well-suited to forming a tight dimer probably because the SL1 dimer-inducing element is located at the very 3′-end of this fragment (Figure 1).

Here we demonstrate that large HIV-2 RNAs encompassing the complete leader region cannot efficiently form tight dimers *in vitro*. Indeed, the low level of tight dimer we observed with the 1−561 RNA is probably not mediated by SL1 in the absence of NCp7 based on two lines of evidence. First, these dimers are not inhibited by an antisense oligonucleotide directed against the SL1, to which the 1−444 RNA tight dimers are very sensitive (*17*). Second, as pointed out by Laughrea *et al*., some stem−loop structures may have a melting temperature close to the incubation temperature of 55 °C and could occasionally switch from intrastrand to interstrand base pairing (*35*). This might also be the case for HIV-2, since, for example, the tight dimer level was lower when the TAR and poly(A) signal structures were missing (Figure 4B, compare lanes 1 and 2 to lanes 3−5).

Using RNAs truncated at their 5′- or 3′-ends and using compensatory site-directed mutagenesis, we found that two elements, between nucleotides 189−196 and 543−550, prevent the formation of SL1-dependent tight dimers of HIV-2 leader RNA. A similar study by Dirac *et al*. (*16*) approximated the border of an upstream dimer-interfering element to between nucleotides 507 and 527, since they did not observe tight dimerization for RNAs longer than 527 nucleotides. There are several experimental differences that could explain the discrepancy between their results and our own. First, the dimerization protocols are somewhat different (a thorough comparison was published in ref *17*). Briefly, in the study presented here, the denatured RNA was incubated at a constant temperature of 55 °C to induce tight dimerization; the Dirac *et al*. study used a slow-cooling protocol from 65 °C to room temperature. Second, in our hands, the optimal dimerization yield with 1−444 RNA was higher (compare refs *16* and *19* to this paper). To resolve this discrepancy, we analyzed the kinetics of tight dimer formation for the RNAs that were able to form a substantial level of tight dimer at 50, 55, or 60 °C in Dirac dimer buffer (i.e., 1−444, 1−526, 1−541, and 1−546 RNAs). We observed that sequences downstream of SL1 influence the tight dimerization through a decrease in the dimerization rate. Thus, we think the difference in tight dimerization yield between the 1−507 and 1−527 RNAs seen by Dirac *et al*. is due to the additive effects of differences in the overall dimerization levels and the kinetic influence of sequences upstream of nucleotide 546 on the SL1-dependent dimerization.

Effects of sequences upstream and downstream of the major splice donor site on the dimerization process have been demonstrated in HIV-1 as well. The HIV-1 *Mal* isolate SL1-dependent dimerization is influenced by sequences located downstream of SL1. The thermal stability and yield of the dimers for a large RNA in the presence of the downstream sequences were increased by 10 °C and 18%, respectively (*34*). A similar region in HIV-1 *Lai* isolate increased the tight dimerization rate by a factor of 2−3 but did not change the thermal stability of the SL1-dependent dimers (*36*). Thus, the downstream sequences of the leader RNA in HIV-1 and HIV-2 have opposite effects on SL1-mediated dimerization. There is a strong negative influence of sequences downstream (and upstream) of the major splice donor site on the SL1-mediated HIV-2 RNA dimerization. This is reminiscent of the interference between the non-native SL1 loop sequence and the 3′-dimer linkage structure in the *in vivo* replication and *in vitro* dimerization of HIV-1 *Lai* RNA (*35*, *37*).

Our data suggest that a long-range base pairing interaction prevents the use of the SL1 sequence for tight dimerization. We believe there is competition between intramolecular and intermolecular interactions of the SL1 structure of HIV-2 leader RNA. An example of an energetically favorable secondary structure in which SL1 is sequestered intramolecularly is shown in Figure 8. Base pairing between nucleotides 189−196 and 543−550 favors an intramolecular folding of the SL1 sequence, preventing its use in an intermolecular SL1−SL1 interaction. We cannot formally rule out the possibility of a direct interaction between the upstream and downstream interfering elements and the SL1 sequence. However, computer-assisted folding of the 1−561 RNA could not demonstrate such an interaction (*26*, *27*; J.-M. Lanchy and J. S. Lodmell, data not shown). Moreover, analysis of HIV-2 and SIV aligned sequences in the *HIV Sequence Compendium 2001* showed a perfect conservation of all nucleotides involved in the long-range base pairing (*38*). Although the *gag* initiation and subsequent codons are highly conserved because of the selective pressure on translation and post-translational modifications of the Gag protein, it is interesting to find 100% conservation in the region of residues 189−196. The only role so far suggested for this sequence may be as part of the downstream GU/U-rich element cis-acting signal required for mammalian polyadenylation (*39*).

It appears to be significant that one of the sequences involved in the long-range interaction proposed here includes the *gag* initiation codon. Experiments by the Lever group showed that HIV-2 selects its genomic RNA for encapsidation cotranslationally (*20*). Two elements seem to mediate this activity: the nucleocapsid domain of the Gag protein and the sequence of residues 380−408 located just upstream of the SL1 sequence in the leader RNA region, called the encapsidation signal or Ψ (Figure 8) (*20*). Mutagenesis studies have shown that retroviral encapsidation and dimerization elements overlap *in vivo* (for a review, see ref *40*). This functional overlap may be explained by a structural overlap. Computer-assisted folding of the 1−561 RNA without any constraint showed two main foldings for the SL1 domain: either as an individual stem−loop structure, as

described by Berkhout *et al*. (*29*), or involved in a secondary structure with the core HIV-2 RNA encapsidation signal Ψ (Figure 8). Since the initiating ribosome complex reads the initiation codon of *gag* and surrounding nucleotides, it may disrupt the long-range interaction and allow conformational changes of the leader RNA region. After translation of the nucleocapsid domain, this domain may preferentially interact with its own messenger RNA and promote more extensive conformational changes, thus modulating dimerization and encapsidation. In fact, evidence along these lines has been presented *in vitro* for the Gag precursor (*41*−*43*) and for the mature nucleocapsid protein (*5*, *18*, *24*, *25*, *41*, *44*). We showed in this study that the nucleocapsid protein is able to promote the formation of SL1-dependent HIV-2 RNA tight dimers *in vitro*. It would be of interest to determine the conformation of the core encapsidation and dimerization sequences prior to and after translation or encapsidation *in vivo*. A similar relationship between translation and encapsidation has recently been elucidated in HIV-1, even though the cis preference of the Gag protein for encapsidation of its own messenger RNA was not absolute and could be overcome (*45*, *46*).

Although there are many questions that remain to be answered, it is already clear that the 5′-leader region of HIV-2 and other retroviral RNAs is replete with functionality. Furthermore, the emerging view of the complex and switchable structure variations possible *in vitro* in the 5′-leader region strongly implicates it as a key *regulatory* element *in vivo*. The complete characterization of dimerization and encapsidation as well as other regulatory roles for this region will require continued dissection of these closely linked processes using a variety of *in vitro* and *in vivo* techniques.

ACKNOWLEDGMENT

We gratefully acknowledge John Marino, Roland Marquet, Jean-Christophe Paillart, and Hector Valtierra for critical reading of the manuscript and helpful suggestions. The following reagent was obtained through the AIDS Research and Reference Reagent Program, Division of AIDS, NIAID, NIH: p83-2 from Dr. Ronald Desrosiers (*21*). The pROD10 plasmids from Drs. J.-M. Bechet and A. M. L. Lever were obtained from the Centralised Facility for AIDS Reagents supported by EU Programme EVA (Contract QLK2-CT-1999-00609) and the U.K. Medical Research Council.

REFERENCES

1. Bender, W., and Davidson, N. (1976) *Cell 7*, 595−607.
2. Hoglund, S., Ohagen, A., Goncalves, J., Panganiban, A. T., and Gabuzda, D. (1997) *Virology 233*, 271−279.
3. Laughrea, M., Shen, N., Jette, L., Darlix, J. L., Kleiman, L., and Wainberg, M. A. (2001) *Virology 281*, 109−116.
4. Fu, W., Gorelick, R. J., and Rein, A. (1994) *J. Virol. 68*, 5013−5018.
5. Darlix, J. L., Gabus, C., Nugeyre, M. T., Clavel, F., and Barre-Sinoussi, F. (1990) *J. Mol. Biol. 216*, 689−699.
6. Laughrea, M., and Jette, L. (1994) *Biochemistry 33*, 13464−13474.
7. Skripkin, E., Paillart, J. C., Marquet, R., Ehresmann, B., and Ehresmann, C. (1994) *Proc. Natl. Acad. Sci. U.S.A. 91*, 4945−4949.
8. McBride, M. S., and Panganiban, A. T. (1996) *J. Virol. 70*, 2963−2973.
9. Jossinet, F., Lodmell, J. S., Ehresmann, C., Ehresmann, B., and Marquet, R. (2001) *J. Biol. Chem. 276*, 5598−5604.
10. Laughrea, M., and Jette, L. (1996) *Biochemistry 35*, 1589−1598.
11. Muriaux, D., Fosse, P., and Paoletti, J. (1996) *Biochemistry 35*, 5075−5082.
12. Shubsda, M. F., McPike, M. P., Goodisman, J., and Dabrowiak, J. C. (1999) *Biochemistry 38*, 10147−10157.
13. Clever, J. L., Wong, M. L., and Parslow, T. G. (1996) *J. Virol. 70*, 5902−5908.
14. Haddrick, M., Lear, A. L., Cann, A. J., and Heaphy, S. (1996) *J. Mol. Biol. 259*, 58−68.
15. Paillart, J. C., Skripkin, E., Ehresmann, B., Ehresmann, C., and Marquet, R. (1996) *Proc. Natl. Acad. Sci. U.S.A. 93*, 5572−5577.
16. Dirac, A. M., Huthoff, H., Kjems, J., and Berkhout, B. (2002) *Nucleic Acids Res. 30*, 2647−2655.
17. Lanchy, J. M., and Lodmell, J. S. (2002) *J. Mol. Biol. 319*, 637−648.
18. Takahashi, K., Baba, S., Koyanagi, Y., Yamamoto, N., Takaku, H., and Kawai, G. (2001) *J. Biol. Chem. 276*, 31274−31278.
19. Dirac, A. M., Huthoff, H., Kjems, J., and Berkhout, B. (2001) *J. Biol. Chem. 276*, 32345−32352.
20. Griffin, S. D., Allen, J. F., and Lever, A. M. (2001) *J. Virol. 75*, 12058−12069.
21. Gibbs, J. S., Regier, D. A., and Desrosiers, R. C. (1994) *AIDS Res. Hum. Retroviruses 10*, 343−350.
22. Deleted on proof.
23. Marquet, R., Paillart, J. C., Skripkin, E., Ehresmann, C., and Ehresmann, B. (1994) *Nucleic Acids Res. 22*, 145−151.
24. Rist, M. J., and Marino, J. P. (2002) *Biochemistry 41*, 14762−14770.
25. Muriaux, D., De Rocquigny, H., Roques, B. P., and Paoletti, J. (1996) *J. Biol. Chem. 271*, 33686−33692.
26. Mathews, D. H., Sabina, J., Zuker, M., and Turner, D. H. (1999) *J. Mol. Biol. 288*, 911−940.
27. Zuker, M., Mathews, D. H., and Turner, D. H. (1999) in *RNA Biochemistry and Biotechnology* (Barciszewski, J., and Clark, B. F. C., Eds.) pp 11−43, Kluwer Academic Publishers, Dordrecht, The Netherlands.
28. Rhim, H., and Rice, A. P. (1994) *Virology 202*, 202−211.
29. Berkhout, B., and Schoneveld, I. (1993) *Nucleic Acids Res. 21*, 1171−1178.
30. Voss, T. G., Fermin, C. D., Levy, J. A., Vigh, S., Choi, B., and Garry, R. F. (1996) *J. Virol. 70*, 5447−5454.
31. Jossinet, F., Paillart, J. C., Westhof, E., Hermann, T., Skripkin, E., Lodmell, J. S., Ehresmann, C., Ehresmann, B., and Marquet, R. (1999) *RNA 5*, 1222−1234.
32. Paillart, J. C., Westhof, E., Ehresmann, C., Ehresmann, B., and Marquet, R. (1997) *J. Mol. Biol. 270*, 36−49.
33. Muriaux, D., Girard, P. M., Bonnet-Mathoniere, B., and Paoletti, J. (1995) *J. Biol. Chem. 270*, 8209−8216.
34. Paillart, J. C., Marquet, R., Skripkin, E., Ehresmann, B., and Ehresmann, C. (1994) *J. Biol. Chem. 269*, 27486−27493.
35. Laughrea, M., and Jette, L. (1997) *Biochemistry 36*, 9501−9508.
36. Laughrea, M., and Jette, L. (1996) *Biochemistry 35*, 9366−9374.
37. Laughrea, M., Shen, N., Jette, L., and Wainberg, M. A. (1999) *Biochemistry 38*, 226−234.
38. Kuiken, C., Foley, B., Hahn, B., Marx, P., McCutchan, F., Mellors, J., Wolinsky, S., and Korber, B. (2001) *HIV Sequence Compendium 2001*, Theoretical Biology and Biophysics Group, Los Alamos National Laboratory, Los Alamos, NM.
39. Levitt, N., Briggs, D., Gil, A., and Proudfoot, N. J. (1989) *Genes Dev. 3*, 1019−1025.
40. Greatorex, J., and Lever, A. (1998) *J. Gen. Virol. 79*, 2877−2882.
41. Damgaard, C. K., Dyhr-Mikkelsen, H., and Kjems, J. (1998) *Nucleic Acids Res. 26*, 3667−3676.
42. Feng, Y. X., Campbell, S., Harvin, D., Ehresmann, B., Ehresmann, C., and Rein, A. (1999) *J. Virol. 73*, 4251−4256.
43. Zeffman, A., Hassard, S., Varani, G., and Lever, A. (2000) *J. Mol. Biol. 297*, 877−893.
44. Lapadat-Tapolsky, M., Pernelle, C., Borie, C., and Darlix, J. L. (1995) *Nucleic Acids Res. 23*, 2434−2441.
45. Poon, D. T., Chertova, E. N., and Ott, D. E. (2002) *Virology 293*, 368−378.
46. Liang, C., Hu, J., Russel, R. S., and Wainberg, M. A. (2002) *AIDS Res. Hum. Retroviruses 18*, 1117−1126.

BI0271190